analytical chemistry

Technical Note

pubs.acs.org/ac

Disposable Attenuated Total Reflection-Infrared Crystals from Silicon Wafer: A Versatile Approach to Surface Infrared Spectroscopy

Engin Karabudak,*,† Recep Kas,*,‡ Wojciech Ogieglo,§ Damon Rafieian,∥ Stefan Schlautmann,† R. G. H. Lammertink,∥ Han J. G. E. Gardeniers,† and Guido Mul‡

†Mesoscale Chemical Systems Group, ‡Photo Catalytic Synthesis Group, §Membrane Technology Group, ∥Soft Matter, Fluidics and Interfaces, MESA+ Institute for Nanotechnology, University of Twente, P.O. Box 217, 7500 AE Enschede, The Netherlands

Ⓢ *Supporting Information*

ABSTRACT: Attenuated total reflection-infrared (ATR-IR) spectroscopy is increasingly used to characterize solids and liquids as well as (catalytic) chemical conversion. Here we demonstrate that a piece of silicon wafer cut by a dicing machine or cleaved manually can be used as disposable internal reflection element (IRE) without the need for polishing and laborious edge preparation. Technical aspects, fundamental differences, and pros and cons of these novel disposable IREs and commercial IREs are discussed. The use of a crystal (the Si wafer) in a disposable manner enables simultaneous preparation and analysis of substrates and application of ATR spectroscopy in high temperature processes that may lead to irreversible interaction between the crystal and the substrate. As representative application examples, the disposable IREs were used to study high temperature thermal decomposition and chemical changes of polyvinyl alcohol (PVA) in a titania (TiO_2) matrix and assemblies of 65−450 nm thick polystyrene (PS) films.

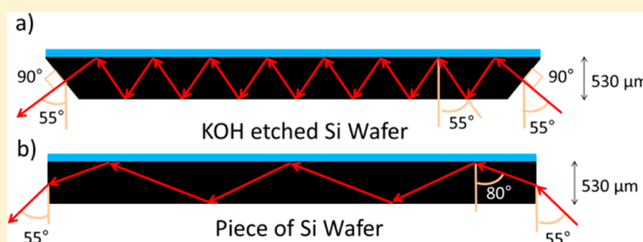

Traditional analytical techniques for surface analysis such as X-ray photoelectron spectroscopy (XPS), low-energy electron diffraction (LEED), scanning tunneling microscopy (STM), and field emission microcopy (FEM) operate in ultrahigh vacuum and therefore require removal of the solvent in which the surface was prepared, which may cause changes in the surface characteristics.[1,2] Attenuated total reflection-infrared spectroscopy (ATR-IR) is a nondestructive and relatively easy technique to study the chemical composition of samples. The short penetration depth of the light into the sample is its most important advantage over transmission IR spectroscopy. This allows studies of compounds dissolved in strongly absorbing media such as water.[3] ATR-IR spectroscopy has been widely used to analyze solid−liquid interfaces and to determine mechanistic aspects of liquid phase reactions.[4−8]

The crystals employed in commercial ATR-IR cells allow a wide range of chemicals to be analyzed. For strong acids, bases, or oxidizing agents, typically diamond or diamond like coatings on internal reflection elements (IREs) are applied[9,10] and such crystals are also commercially available. Almost any kind of thin film coated on IREs can be analyzed, although strong adhesion due to chemical reaction or interdiffusion established by high temperature annealing may complicate cleaning of the IREs after analysis, and possibly the crystal surface might become damaged by the harsh cleaning conditions necessary.[11] A large stock of IREs is usually not available in most laboratories, which restricts parallel preparation and fast screening of a series of thin films, and does not allow keeping the films for a long time for reinspection or further characterization. Shifting from costly commercial IREs to conventional, easily accessible Si wafers or wafer pieces might alleviate the importance of cleaning and allow multiple samples to be prepared for analysis at the same time. Particularly in areas where silicon wafers are used as substrates and model surfaces, disposable IREs appear of interest.

Si is one of the most attractive materials to be used in infrared spectroscopy because processing of silicon is well developed in the field of microelectronics and micro-electromechanical systems (MEMS). This has led to the use of silicon to construct microreactors and micro analytical devices.[12,13] In addition, silicon crystals are commonly used as substrates to deposit thin films by different methods such as sol−gel deposition, layer-by-layer techniques, chemical vapor deposition (CVD), plasma-enhanced chemical vapor deposition (PECVD), wafer bonding, etc.[14−18] Si wafers are used frequently as a substrate when near-to-atomically smooth surfaces are needed to characterize coatings with, for example, ellipsometry or atomic force microscopy (AFM). Functionalization of silicon surfaces is very well established.

Commercial Si IREs are made of thick silicon and they require extensive polishing of their side edges. Micromachined silicon, such as KOH etched as shown in Figure 1a, is very suitable as an IRE,[19−23] with the advantage that also the spectral region below 1500 cm^{-1} can be analyzed as a result of

Received: August 10, 2012
Accepted: December 4, 2012
Published: December 4, 2012

ACS Publications © 2012 American Chemical Society

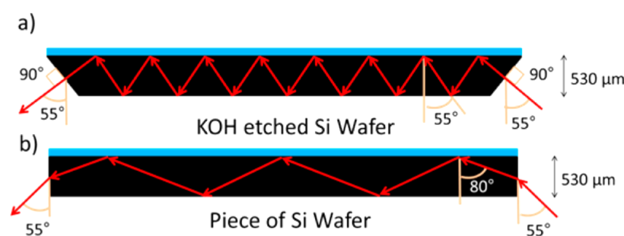

Figure 1. Schematic representation of a piece of silicon, when employed as an IRE. Differences in light propagation for angled edges prepared by KOH etching and straight edges by simple cutting are compared.

the decreasing distance that an incident IR beam travels through the silicon crystal.[19,24,25] However, creation of well-defined edges requires deposition of a protective layer (usually a coating prepared by sputtering or CVD), photolithography, and wet etching, and most importantly, quite accurate alignment to crystallographic directions, time and money consuming methods which may not be readily accessible to the majority of laboratories. In conclusion, a need exists for simplified IREs, which can be used in a disposable manner, if required.

The consequence of not having a well-defined edge might be a significant loss of signal due to suboptimal conditions to couple in the infrared light effectively. Considering the Rayleigh criterion, the characteristic roughness must be smaller than 0.4 μm in order to have optical transparency in the mid-infrared region. In this study, we experimentally prove that the surface of the side wall of the Si wafer that is cut by a dicing machine or cleaved manually is smooth enough to obtain useful IR spectra, when inserted in a specially designed sample holder. We will discuss some fundamental aspects of conducting ATR-IR spectroscopy with these disposable IREs and their limitations. As proof of concept, we have analyzed titania-polymer composite films as an example of highly adhesive coatings treated at high temperatures. In addition to the above example, polystyrene (PS) films in a series of increasing thickness were studied to validate Si piece-to-piece reproducibility and to establish whether the increasing thickness will lead to a linearly increasing spectral absorption.

EXPERIMENTAL SECTION

ATR-IR Setup. A p-doped CZ (resistivity 8 Ω cm) 4-in. standard[26] Si wafer was used as a substrate to prepare IREs. A total of 16 pieces with sizes of 15 mm × 20 mm from this Si wafer were cut by a dicing machine (Disco DAD 32, 300 μm thick Thermocarbon T dicing blade), unless otherwise stated.

A four mirror system containing a holder for the Si pieces[22,23] was inserted into a Bruker Vertex 70 infrared spectrometer. The infrared beam from this spectrometer is focused precisely onto the edge of the 530 μm thick Si wafer, with a defined angle of 55°, as shown in Figure 1. Spectra were taken with integration time of 30 s, resolution of 4 cm^{-1}, and beam aperture of 8 mm.

Titania-PVA composite films and PS films were prepared by a spin coating process. Details of preparation of these thin films are given in the Supporting Information. The thickness of the Titania-PVA films was measured by surface profilometry (Metrology VEECO, Dektak 150). For PS films, a M-2000X spectroscopic ellipsometer (J. A. Woolam, Co., Inc.) was used to measure film thickness with a maximum error of ±2 nm. Equation 1 is used to calculate the effective penetration depth of the light into the polystyrene films.

$$d_p = \frac{\frac{\lambda}{n_{Si}}}{2\pi\sqrt{\left(\sin^2\theta - \left(\frac{n_{em}}{n_{Si}}\right)^2\right)}} \quad (1)$$

where d_p is the penetration depth, λ the wavelength, n_{em} is the refractive index of the polystyrene film (1.59); n_{Si} the refractive index of silicon (3.44), and θ the incidence angle of internal reflection (80°).

RESULTS AND DISCUSSION

Before demonstrating the high quality spectra that can be obtained with diced Si pieces, we will first give a detailed discussion of the pros and cons in terms of optical properties of the angled (in our case, KOH-etched) and straight edge Si wafer pieces.

A first issue is the effect of light refraction and reflection at the crystal edge with a specific angle. As shown in Figure 1, IR light hits the side wall of the KOH etched and straight edge Si wafer with an angle of 90° and 55°, respectively. In literature, it is common practice to assign a single value to the incident angle, but in this study we assume a variation of ±10° in the incident angle. In the case of KOH etched edges,[19−23] infrared light enters with an angle of 90° (±10°) and there will be no refraction for the 90° incident angle, but for angles other than 90° there will be refraction according to Snell's law ($n_1 \sin\theta_1 = n_2 \sin\theta_2$ and $n_{air} = 1$; $n_{Si} = 3.44$). Since light is focused on the edge of a diced Si wafer with an angle of 55° (±10°) (Figure 1b), there is refraction for all incident angles. Consequently, light internally reflects with an angle of 80° (±2.5°) from the top and bottom surface of the straight-edge Si wafer and 55° (±2.9°) from the top and bottom surface of KOH etched Si. As indicated in Figure 1, for the straight-edge sample three reflections on the top surface will take place inside the 2 cm long Si wafer piece, while for the optimized KOH-etched sample with the same length 13 internal reflections will occur on the top surface. It is important to note that the light with an angle of refraction of 80°(±2.5°) cannot make even one reflection in a 5 mm thick straight-edge crystal, which is the typical thickness for commercial crystals. This reduction in the number of reflections will evidently lead to a lower signal-to-noise ratio. A wider angle internal reflection results in a lower penetration depth of IR light into the sampled medium, which on the other hand increases the relative contribution in the recorded spectrum of the region close to the silicon surface, which can be an important advantage in interface studies. It is also worth noting that a high number of internal reflections is not always desired, an example being surface enhanced infrared spectroscopy.[27]

A second point of discussion is the total intensity of IR light entering the Si wafer pieces as a function of the edge profile. Fresnel equations for perpendicularly and parallel polarized light are given in equations SI1 and SI2 of Supporting Information. Calculated reflectance values for the S and P polarized light components as a function of incident angle are shown in Figure 2. The total intensity is plotted by averaging the reflected intensities of the polarized light. With an incident angle of 35° (±10°), we find an average reflectance value of 0.30, in which the intensity of the incident light decreases to 30% of its initial value due to reflection. Interestingly, an

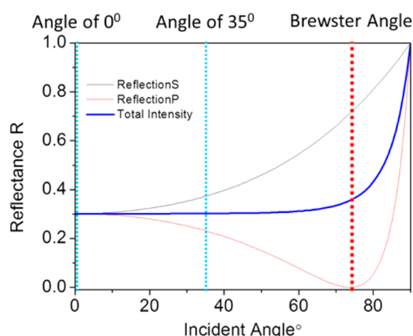

Figure 2. Reflectance of light from the air−silicon interface, as a function of incident angle.

incident angle of 0° (±10°) will also give 30% reflection. The main conclusion of this exercise is that the amount of light coupled into the wafer with the straight edge is just as much as for the optimized angle, since in both cases the incident angle is below the Brewster angle. However, the ratio of the components of polarized light changes and this is the main difference between disposable Si IREs in comparison to KOH etched Si IREs. This will affect the band intensities of oriented molecules; however, we assume that in the majority of samples in laboratories around the world, and certainly the molecules in the samples that we are studying here (PS and Titania-PVA thin films), will have no regular orientation. So using disposable IREs does not have any effect on the spectral appearance of the systems studied here and in fact might open new possibilities for studying oriented samples.

We would like to elaborate somewhat more on the differences between disposable IREs (or in general wafer-based silicon IREs[19−23]) and commercial Si IREs. As already touched upon above, disposable IREs, if obtained from 100 mm diameter silicon {100} wafers, have a thickness of ~0.5 mm and commercial Si IREs typically have a thickness of 5 mm. In our setup, the incoming IR light has a beam diameter of 8 mm, and the four mirror setup[22] focuses the light with a spot size of 5 mm on the side-wall of a disposable IRE. To be more precise, a 5 mm beam has an area of 19.6 mm^2, but only a 5 mm × 0.5 mm (2.5 mm^2) portion of this initial IR light hits the side wall. With 30% reflection, we calculate that only 8% of the original light beam will enter the Si wafer (it is very likely that the coupled intensity is more than these 8% since the intensity of the focused beam will be higher in the center). In infrared spectroscopy it is quite common that only a small portion of the initial light will eventually reach the detector, also with commercial systems like diffuse reflectance setups.[28] Nevertheless, as will be discussed later, this intensity is enough to study ultrathin films. After the refraction process, the coupled light is internally reflected from the interface of the silicon piece and excites molecular vibrations in its evanescent wave on a certain area which depends on the size of the collected beam. The total intensity of the light coupled into the silicon crystal would be maximized if our four mirror setup would focus the light in a spot size of 0.5 mm diameter instead of 5 mm, but this has the drawback that the sampled area would be smaller, which would eventually lead to a decrease in excited vibrations at the surface. In other words, decreasing the beam size decreases surface sensitivity, whereas increasing the beam size decreases the intensity of the light coupled to the Si wafer. For this reason we have optimized our four mirror setup in order to focus the IR light into a diameter of 5 mm.

In Figure SI4 (see the Supporting Information), three background spectra are given for a KOH-etched Si wafer piece (blue), a straight-edge Si wafer piece (red), and as a reference a single beam spectrum obtained without the sample holder (black). Without the sample holder, our detector saturates when the beam aperture is larger than 0.5 mm, which is why the single beam spectrum is taken with a 0.5 mm beam size. On the other hand, in order to get sufficient intensity from Si wafer-based IREs, as explained before, our beam aperture is adjusted to 8 mm for KOH etched IREs and straight edge disposable IREs. Our spectrometer measures the total intensity of light reaching the detector by using an analog to digital converter. This converter has a dynamic range of 0−32 000 counts. In the single beam spectrum, obtained with 0.5 mm beam aperture, 30 000 counts were obtained, the KOH etched Si piece in the four mirror setup gives 25 000 counts, whereas the straight-edge Si pieces gives values around 14 000 counts. The difference in counts between the latter two silicon samples can be explained by the difference in surface area of the side walls into which the light is coupled, which theoretically should give a ratio of sin(55°) = 0.82 for the intensity of the straight-edge with respect to the KOH etched silicon specimen. The real ratio is somewhat lower, which probably can be attributed to the higher roughness of the diced (or cleaved) side-wall.

Background spectra of the empty cell, KOH etched, and straight-edge disposable Si IREs show a similar pattern above 1500 cm^{-1} as shown in Figure 3, except that in the spectra

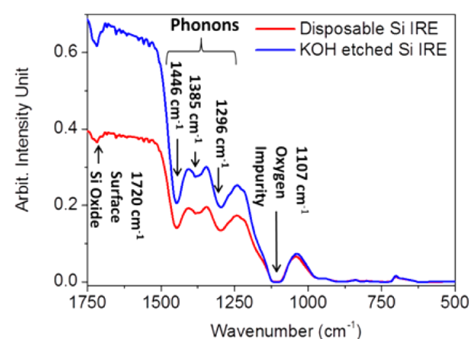

Figure 3. Background spectra of a KOH etched and straight-edge Si IRE wavenumber range 1750 cm^{-1} to 400 cm^{-1}. (The full range is given in Figure SI4 in the Supporting Information.)

taken with Si IRE background there is a surface native oxide peak at 1720 cm^{-1}. Below 1500 cm^{-1} three different intensity regions can be distinguished: (i) Between 1500 cm^{-1} and 1200 cm^{-1}, three phonon peaks[23] are present at 1448 cm^{-1} (3TO), 1378 cm^{-1} (3TO + LO), and 1302 cm^{-1} (2TO +LO). Normally in 5 mm commercial thick Si IREs, these phonon peaks absorb all IR light, which makes spectral analysis below 1500 cm^{-1} impossible.[29] Using thinner Si IREs helps in this respect, since the phonon band absorption decreases dramatically with wafer thickness.[30] (ii) Below 1200 cm^{-1}, a region (1089 cm^{-1} to 1120 cm^{-1}) is present in which a strong interstitial oxygen (Si−O) vibration with a peak at 1107 cm^{-1} absorbs all IR intensity. Interstitial oxygen is a trace element resulting from the production process of the silicon wafers, well-known for Czochralski (CZ) wafers as used in our study. To avoid such impurities, higher purity (but more expensive) float zone (FZ) wafers should be used. (iii) Below 1089 cm^{-1} down to 908 cm^{-1} and in the range of 727 cm^{-1} and 620 cm^{-1},

again some IR absorption takes place, but in our work we did not further use this region.

Titania-PVA Films. The infrared spectra of the titania-PVA composite films after various temperature treatments are presented in Figure 4. The polymer itself contains unhydrolyzed acetate groups or residual sodium acetate remaining from the hydrolysis step of polyvinyl acetate, which is a common observation during the synthesis of PVA[31,32](Figure SI2 in the Supporting Information). Decomposition and mass loss of PVA occurs readily between 200 and 300 °C.[33] In order to see the changes in this temperature range, the coated substrates were annealed at 250 °C for 20 min. Because of dehydration and oxidation of PVA molecules, the infrared spectrum of the annealed samples show decreasing intensities of C−H and O−H bonds. After annealing at 250 °C, the color of the films turns to brown, which is an indication of formation of chromophoric carbonyl compounds with nonselective absorption bands in the visible and near-infrared region.[34] In the first thermal cycle (comp2), the intensity of the peaks in the carbonyl region decreases and changes into a single peak at 1715 cm^{-1}. In addition, a new peak emerges centered around 1600 cm^{-1}. The disappearance of the band at 1570 cm^{-1} is most likely due to evaporation and decomposition of volatile acetic acid. After the second cycle, the intensities of the bands corresponding to O−H and C−H modes have further decreased whereas the bands located at 1715 cm^{-1} and 1600 cm^{-1} have slightly increased. These bands are assigned to C=O and C=C stretching modes of unsaturated carbonyl compounds, which are formed by dehydration.[35] In order to detect the organic content after sintering, the film was also annealed at 500 °C for 2 h. The color of the films turned to white, which indicates the removal of the carbonaceous compounds. However even after sintering, the band at 1249 cm^{-1} remains visible. This can most likely be attributed to the formation of C−O−Ti bonds, due to reaction of PVA with the titania gel, which increases the thermal stability of the organic groups.[36]

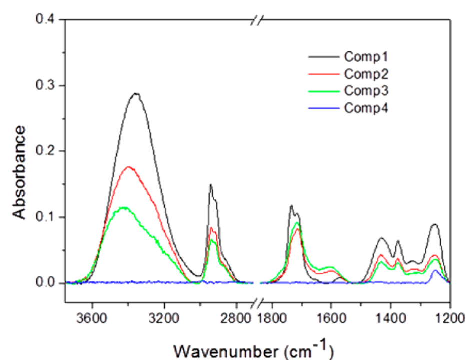

Figure 4. ATR-IR spectra of titania-PVA composite films. Comp1, after baking at 120 °C; Comp2, after the 1st cycle, i.e., 20 min annealing at 250 °C; Comp3, after the 2nd cycle of and an additional 20 min of annealing at 250 °C; Comp4, after sintering at 500 °C for 2 h in air.

Ordinarily, the strong adhesion of a ceramic coating to IREs prevents the use of ATR spectroscopy to characterize the transformations leading to its formation, simply because the crystals used cannot be properly cleaned. While diamond crystals actually can be used for studying high temperature processes, certainly diamond does not allow efficient simultaneous preparation of the films. The attractiveness of the usage of the disposable ATR-IR crystals, in this first example used to study formation of titania-PVA coatings, lies in the simultaneous processing of multiple samples at high temperatures.

Polystyrene Films. Polystyrene was chosen to study the linear relation between spectral intensity and film thickness, because it is a well-studied macromolecular system frequently employed in fundamental research (see the Supporting Information for details). We have prepared PS thin films in the thickness range 60−450 nm to analyze spectral intensities for films around and below the evanescent wave decay length. In Figure SI5 in the Supporting Information, it can be seen that the intensity of the PS thin film peaks increases as a function of increasing thickness. The absorbance at a certain wavenumber or the area under an infrared peak is proportional to the number of the chemical bonds excited at that wavelength. Therefore, ATR-IR is often applied qualitatively and semi-quantitatively to determine compositional changes.[37,38] Since the evanescent wave intensity shows an exponential decay as a function of depth into the sample, the absorbance-concentration vs thickness should not be linear. However, for thin films with thickness considerably smaller than the evanescent wave decay length, the thickness or concentration might show linear behavior.[39,40] In Figure 5, the thickness is plotted against absorption intensity of the C−H stretching vibration at 2923 cm^{-1}. With eq 1, an incoming angle of 55° (±10°) and an internal reflection angle of 80°(±2.5°), the penetration depth at 2923 cm^{-1} for PS films can be calculated to be 182 (±1) nm. However it is important to note that the actual sampling depth can be on the order of 3 times the penetration depth.[41] The absorbance-thickness graph shows a linear relation with a regression value of 0.9997 below 150 nm and slightly deviates from linearity when the thickness of the films increases. The linear relation shows that the intensity is hardly a function of the silicon substrate used. This is important because any difference in roughness on the side walls of the Si wafer may change the incidence angle or promote scattering which will eventually change the intensity of the light. Our simple method of Si preparation thus allows the direct comparison of spectra collected from different Si pieces when it is used as an IRE. At higher thickness, as stated, the nonlinear behavior can be explained by the exponential decay of the evanescent wave intensity as a function of sample thickness.

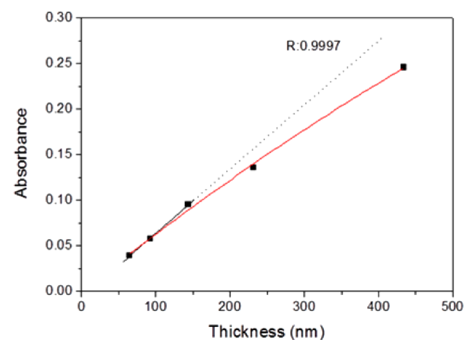

Figure 5. Calibration curve for estimating thickness of polystyrene coatings. The black line is the linear fit for film thicknesses below 150 nm. The dotted line shows the deviation from linearity. The red line is the exponential fit for the complete thickness range.

dx.doi.org/10.1021/ac302299g | *Anal. Chem.* 2013, 85, 33−38

There is no special reason for using a dicing machine to cut the Si wafers, except the fact that the machine is able to cut more precise specimens that fit into a sample holder. We also manually cleaved silicon samples by using a sapphire pen tip (see the Supporting Information, Scheme SI-1) and recorded the spectrum of simple organic compounds, with excellent results (Figure SI-1 in the Supporting Information). Thus, one may even simply cut a piece from a coated large Si wafer for inspection by ATR-IR.

■ CONCLUSIONS

A Si wafer with straight edges prepared by dicing or cleaving can be used as an IRE without any further modification. Thus, relatively cheap and (if desired) disposable IREs for ATR-IR can be obtained, which enables efficient preparation of multiple samples, e.g., to study high-temperature processes in thin films. As a proof of principle, thermal decomposition of PVA in a titania matrix was studied as well as thickness profiling of PS thin films with thicknesses ranging from 65 to 450 nm. Because ATR-IR is nondestructive, the same samples can be used also for SEM inspection or, e.g., in ellipsometric measurements. More importantly, because of the disposable character, original samples can be kept for unrestricted time intervals for further characterization with any other technique. We expect that this mode of easy to use, simple, and cost-effective ATR-IR spectroscopy will significantly contribute to technological and scientific developments in many areas, such as layer-by-layer self-assembly, heterogeneous catalysis, solar to fuel conversion, solar cells, and microfluidics.

■ ASSOCIATED CONTENT

Ⓢ Supporting Information

Related spectra, calibration spectra, and curves. This material is available free of charge via the Internet at http://pubs.acs.org.

■ AUTHOR INFORMATION

Corresponding Author

*E-mail: e.karabudak@utwente.nl (E.K.); r.kas@utwente.nl (R.K.).

Author Contributions

The manuscript was written through contributions of all authors.

Notes

The authors declare no competing financial interest.

■ ACKNOWLEDGMENTS

This project was carried out within the research program of BioSolar Cells, cofinanced by the Dutch Ministry of Economic Affairs, Agriculture and Innovation.

■ REFERENCES

(1) Hind, A. R.; Bhargava, S. K.; McKinnon, A. *Adv. Colloid Interface Sci.* **2001**, *93* (1−3), 91−114.

(2) Karabudak, E.; Demirok, U. K.; Suzer, S. *Surf. Sci.* **2006**, *600* (2), L12−L14.

(3) Vigano, C.; Ruysschaert, J.-M.; Goormaghtigh, E. *Talanta* **2005**, *65* (5), 1132−1142.

(4) Almeida, A. R.; Moulijn, J. A.; Mul, G. *J. Phys. Chem. C* **2008**, *112* (5), 1552−1561.

(5) Burgi, T.; Baiker, A. *Adv. Catal.* **2006**, *50*, 227−283.

(6) Chen, Y. X.; Ye, S.; Heinen, M.; Jusys, Z.; Osawa, M.; Behm, R. J. *J. Phys. Chem. B* **2006**, *110* (19), 9534−9544.

(7) Grunwaldt, J.-D.; Baiker, A. *Phys. Chem. Chem. Phys.* **2005**, *7* (20), 3526−3539.

(8) Mojet, B. L.; Ebbesen, S. D.; Lefferts, L. *Chem. Soc. Rev.* **2010**, *39* (12), 4643−4655.

(9) Janotta, M.; Vogt, F.; Voraberger, H.-S.; Waldhauser, W.; Lackner, J. M.; Stotter, C.; Beutl, M.; Mizaikoff, B. *Anal. Chem.* **2003**, *76* (2), 384−391.

(10) Wharton, D. A.; Petrone, L.; Duncan, A.; McQuillan, A. J. *J. Exp. Biol.* **2008**, *211* (18), 2901−2908.

(11) Muller, G.; Riedel, C. *Appl. Spectrosc.* **1999**, *53* (12), 1551−1555.

(12) Lee, S. J. J.; Sundararajan, N. *Microfabrication for Microfluidics*; Artech House: Boston, MA, 2010.

(13) Reyes, D. R.; Iossifidis, D.; Auroux, P. A.; Manz, A. *Anal. Chem.* **2002**, *74* (12), 2623−36.

(14) Alam, M. J.; Cameron, D. C. *Thin Solid Films* **2000**, *377−378*, 455−459.

(15) Kräuter, G.; Schumacher, A.; Gösele, U.; Jaworek, T.; Wegner, G. *Adv. Mater.* **1997**, *9* (5), 417−420.

(16) Hoppe, H.; Sariciftci, N. S. *J. Mater. Res.* **2004**, *19* (7), 1924−1945.

(17) Erel, I.; Schlaad, H.; Demirel, A. L. *J. Colloid Interface Sci.* **2011**, *361* (2), 477−482.

(18) Erel, I.; Karahan, H. E.; Tuncer, C.; Butun, V.; Demirel, A. L. *Soft Matter* **2012**, *8* (3), 827−836.

(19) Herzig-Marx, R.; Queeney, K. T.; Jackman, R. J.; Schmidt, M. A.; Jensen, K. F. *Anal. Chem.* **2004**, *76* (21), 6476−6483.

(20) Oh, Y. J.; Gamble, T. C.; Leonhardt, D.; Chung, C. H.; Brueck, S. R. J.; Ivory, C. F.; Lopez, G. P.; Petsev, D. N.; Han, S. M. *Lab Chip* **2008**, *8* (2), 251−258.

(21) Oh, Y. J.; Garcia, A. L.; Petsev, D. N.; Lopez, G. P.; Brueck, S. R. J.; Ivory, C. F.; Han, S. M. *Lab Chip* **2009**, *9* (11), 1601−1608.

(22) Karabudak, E.; Mojet, B. L.; Schlautmann, S.; Mul, G.; Gardeniers, H. J. G. E. *Anal. Chem.* **2012**, *84* (7), 3132−3137.

(23) Karabudak, E.; Yuce, E.; Schlautmann, S.; Hansen, O.; Mul, G.; Gardeniers, H. *Phys. Chem. Chem. Phys.* **2012**, *14* (31), 10882−10885.

(24) Weldon, M. K.; Stefanov, B. B.; Raghavachari, K.; Chabal, Y. J. *Phys. Rev. Lett.* **1997**, *79* (15), 2851−2854.

(25) Schumacher, H.; Künzelmann, U.; Vasilev, B.; Eichhorn, K.-J.; Bartha, J. W. *Appl. Spectrosc.* **2010**, *64* (9), 1022−1027.

(26) Ennis, C. P.; Kaiser, R. I. *Phys. Chem. Chem. Phys.* **2010**, *12* (45), 14884−14901.

(27) Ishida, K. P.; Griffiths, P. R. *Anal. Chem.* **1994**, *66* (4), 522−530.

(28) Fuller, M. P.; Griffiths, P. R. *Anal. Chem.* **1978**, *50* (13), 1906−1910.

(29) Vigano, C.; Ruyssehaert, J. M.; Goormaghtigh, E. *Talanta* **2005**, *65* (5), 1132−1142.

(30) Medernach, J. W. Infrared Characterization of Device-Quality Silicon. In *Handbook of Vibrational Spectroscopy*; John Wiley & Sons, Ltd.: New York, 2006.

(31) Shin, J.; Kim, Y.; Lim, Y. M.; Nho, Y. C. *J. Appl. Polym. Sci.* **2008**, *107* (5), 3179−3183.

(32) Shin, J.; Kim, Y.; Lee, K.; Lim, Y. M.; Nho, Y. C. *Radiat. Phys. Chem.* **2008**, *77* (7), 871−876.

(33) Kumar, R. V.; Koltypin, Y.; Cohen, Y. S.; Cohen, Y.; Aurbach, D.; Palchik, O.; Felner, I.; Gedanken, A. *J. Mater. Chem.* **2000**, *10* (5), 1125−1129.

(34) Prosanov, I.; Matvienko, A. *Phys. Solid State* **2010**, *52* (10), 2203−2206.

(35) Tsuchiya, Y.; Sumi, K. *J. Polym. Sci.* **1970**, *7* (PartA-1), 3151−3158.

(36) Yang, W. P.; Huang, S. L. *Sep. Sci. Technol.* **2003**, *38* (16), 4027−4040.

(37) Baptiste, A.; Gibaud, A.; Bardeau, J. F.; Wen, K.; Maoz, R.; Sagiv, J.; Ocko, B. M. *Langmuir* **2002**, *18* (10), 3916−3922.

(38) Korematsu, A.; Takemoto, Y.; Nakaya, T.; Inoue, H. *Biomaterials* **2002**, *23* (1), 263−271.

(39) Freger, V.; Ben-David, A. *Anal. Chem.* **2005**, *77* (18), 6019−6025.

(40) Kane, S. R.; Ashby, P. D.; Pruitt, L. A. *J. Biomed. Mater. Res., Part B: Appl. Biomater.* **2009**, *91B* (2), 613−620.
(41) Mirabella, F. M. *J. Polym. Sci.: Polym. Phys. Ed.* **1983**, *21* (11), 2403−2417.

dx.doi.org/10.1021/ac302299g | *Anal. Chem.* 2013, 85, 33−38